ELECTRICAL CONDUCTIVITY IN Fe_2O_3 AND $CoFe_2O_4$ NANOPARTICLE ARRAYS AND THEIR APPLICATION IN GAS SENSING

Š. Luby[1], M. Benkovičova[1], M. Jergel[1], P. Šiffalovič[1], E. Majková[1], R. Rella[2], S. Capone[2], M. G. Manera[2]

[1] Institute of Physics, Slovak Acad. Sci., Dúbravská cesta 9, 845 11 Bratislava, Slovakia,
[2]Institute of Microelectronics and Microsystems CNR, Via Monteroni, Campus Ecotekne, 73100 Lecce, Italy

E-mail: stefan.luby@savba.sk

Received 29 April 2013; accepted 03 May 2013

1. Introduction

Semiconducting metal oxides belong to the frequently used materials in gas sensing both in environmental protection and in medicine [1]. Amongst the broad variety of well established oxides, like SnO_2, TiO_2, WO_3, ZnO, iron oxide γ-Fe_2O_3 and cobalt – iron oxide $CoFe_2O_4$ attract now attention because of complex magnetic and electric properties and high chemical reactivity. Moreover, innovative sensors are built from nanoparticle (NP) arrays. In comparison with continuous films these devices with high surface/volume ratio are more sensitive [2]. Our sensors are appropriate for oxidizing NO_2 gas. With γ-Fe_2O_3 the response $R = I_{air}/I_{gas}$ (the ratio of the device current in dry air vs. in air mixed with the analysed gas) is 38 at NO_2 concentration C_g = 500 ppb and working temperature $T_w = 350^oC$ [3]. This result is comparable with the top published sensitivities, e.g. R = 8 at C_g = 500 ppb and $T_w = 250^oC$ [4]. With CO and acetone (studied as a marker of diabetes in the patient's breath) the sensitivities are lower [2]. With CO R = 2.8 at C_g = 100 ppm and $T_w = 350^oC$, with acetone R = 1.8 at C_g = 5 ppm at $T_w = 500^oC$. (CO and acetone are reducing gases, hence here $R = I_{gas}/I_{air}$). High sensitivity of NP sensors to oxidizing gases and lower sensitivity to reducing gases was explained by charge carrier self-exhaustion of NPs by surface traps [5]. For the further progress in the field the mechanism of conductivity of NP arrays is of considerable interest. In this paper we summarize the results obtained as a by product of γ-Fe_2O_3 and $CoFe_2O_4$ sensors testing.

2. Experimental

Monodisperse γ-Fe_2O_3 and $CoFe_2O_4$ NPs with the size of 6.4 ± 0.6 and 7.6 ± 0.6 nm, respectively, were synthesized by high-temperature solution phase reaction from metyl acetylacetonates. NPs have a crystalline core (as verified by X-ray diffraction) and a surfactant shell composed from oleic acid and oleylamine [6]. The thickness of surfactant is 1 nm and 0.8 nm for two types of NPs, respectively. Surfactant stops the growth of NPs at a certain size. The self-assembled NP monolayers were prepared by Langmuir-Blodgett technique from the colloid solutions spread on the water subphase in a standard LB trough. M = 1, 2, 4 or 10 NP monolayers (L) were deposited onto auxiliary oxidized Si substrates or onto 2 mm x 2 mm Al_2O_3 sensor substrates equipped with 20 nm Ti/500 nm Pt comb electrodes to read the measuring current and with 20 nm Ti/500 nm Pt meander on the back side for the heating of the structure to a working temperature. Material properties of NPs and arrays were studied by SEM/EDS, GI XRD, GISAXS, XANES and ellipsometry. Before testing samples were treated 20 min in UV reactor equipped with ozone generating (hν = 4.9

and 6.6 eV) mercury lamp to remove the insulating surfactant [6]. Then the samples were stabilized by a long period (4 – 5 days) heating at 450°C – 500°C in dry air to oxidize the initial Fe_3O_4 component in NPs to Fe_2O_3 phase and to decrease the resistivity of NP arrays. The coalescence of NPs was not observed (as a contrary to Co NPs behavior [7]) and NPs were stable even under heating up to 500°C in vacuum, where Fe_2O_3 might be reduced to Fe_3O_4 again [8]. The current through the NP arrays was measured by electrometer at the constant voltage of 10 V between electrodes in dry air. In order to get current > 10 pA the temperature interval 473 K – 773 K (200°C – 500°C) was chosen.

3. Results

SEM pictures of Fe_2O_3 NP array (1 monolayer) on Si are shown in Fig. 1. After surfactant removal the structure is discontinuous with the filler surface fraction < 1. In Fig. 2 we have 10 monolayer LB deposit on Al_2O_3 substrate. The composition of NPs corresponds to Fe_2O_3/Fe_3O_4 mixture. It is transformed to Fe_2O_3 during heating or ageing in air, as we have shown using XANES experiment.

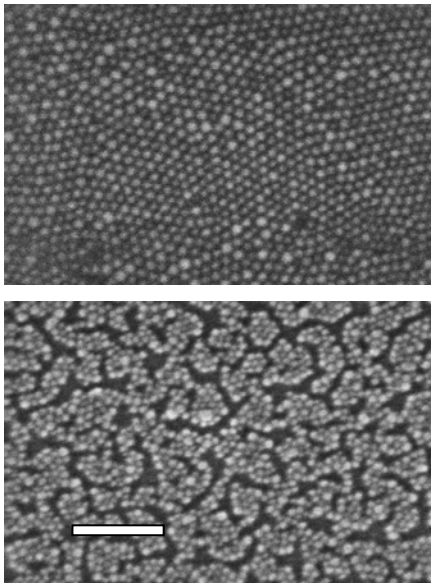

Fig.1: *As dep. (up) and from surfactant stripped L1 NP Fe_2O_3 array (down). Bar = 100 nm.*

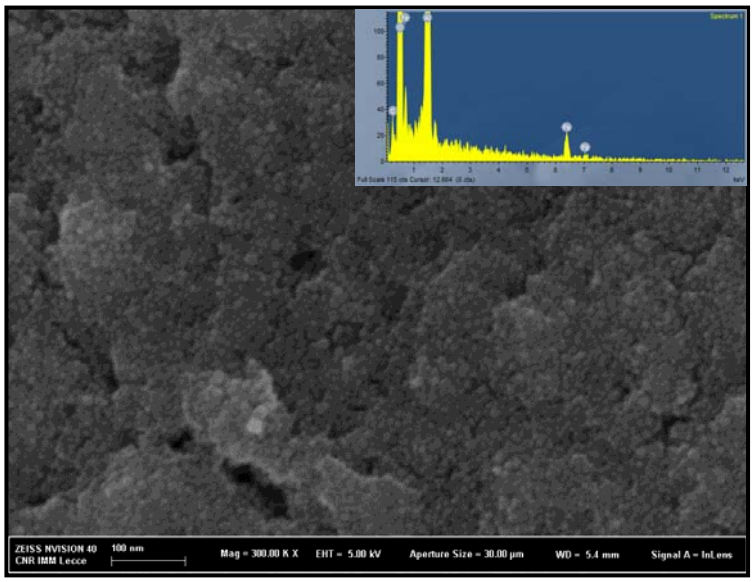

Fig.2: *L10 NP deposit on Al_2O_3 substrate. The coverage follows the roughness of alumina. EDS spectrum is in the corner.*

Electrical properties of samples are summarized in Tab. 1. Here both measured currents and calculated resistivity are shown. The resistivity ρ was obtained from the expression $6.2\text{x}10^{-3}\rho/t$, here t is the thickness of NP deposit and factor $6.2\text{x}10^{-3}$ is calculated from the geometry of the electrode pattern. From ellipsometry it follows that the multilayer thickness is a multiple of the number of layer thickness, i.e. NPs don't sink into the minima between three NPs of the underlying layer. Because of the surfactant stripping the initial thickness was reduced by factors 0.64 and 0.66 for Fe_2O_3 and $CoFe_2O_4$, respectively. They were obtained from SEM pictures. From temperature dependences of the sample current I vs. 1/T (Fig. 3) activation energies E of the thermally activated conductivity were obtained. In four samples (Tab. 1) not an expected n-type, however p-type conductivity was recorded. These samples (not shown here) have two values of activation energy – E, E_1. I vs. 1/T curves are bent and their slopes change at approx. 350°C.

Tab. 1 *LM – samples with M (1, 2, 4, 10) NP monolayers. Fe stays for Fe_2O_3, Co for $CoFe_2O_4$. n, p – types of conductivity. Current I of NP arrays is shown at extreme temperatures 473 K and 773 K. E, E_1 -activation energies of conductivity, ρ - resistivity extrapolated to 293 K using the energy E.*

Sample	Type of conduc-tivity	Current I [A]		E [eV]	E_1[eV]	Resistivity [Ωcm]
		473 K	773 K			293 K
L1 Fe	p	$2.9x10^{-11}$	$2.5x10^{-8}$	0.41	1.04	$1.1x10^{10}$
L2 Fe	n	$3.4x10^{-11}$	$1.2x10^{-9}$	0.41	----	$3.1x10^{10}$
L4 Fe	n	$2.0x10^{-10}$	$5.6x10^{-9}$	0.38	----	$4.7x10^{9}$
L10 Fe	n	$4.6x10^{-8}$	$6.5x10^{-7}$	0.29	----	$1.1x10^{7}$
L1 Co	p	$7.7x10^{-11}$	$5.8x10^{-8}$	0.41	1.10	$4.7x10^{9}$
L4 Co	p	$6.0x10^{-10}$	$1.6x10^{-6}$	0.50	1.20	$9.5x10^{9}$
L10 Co	p	$1.5x10^{-9}$	$5.6x10^{-6}$	0.55	1.25	$2.1x10^{10}$

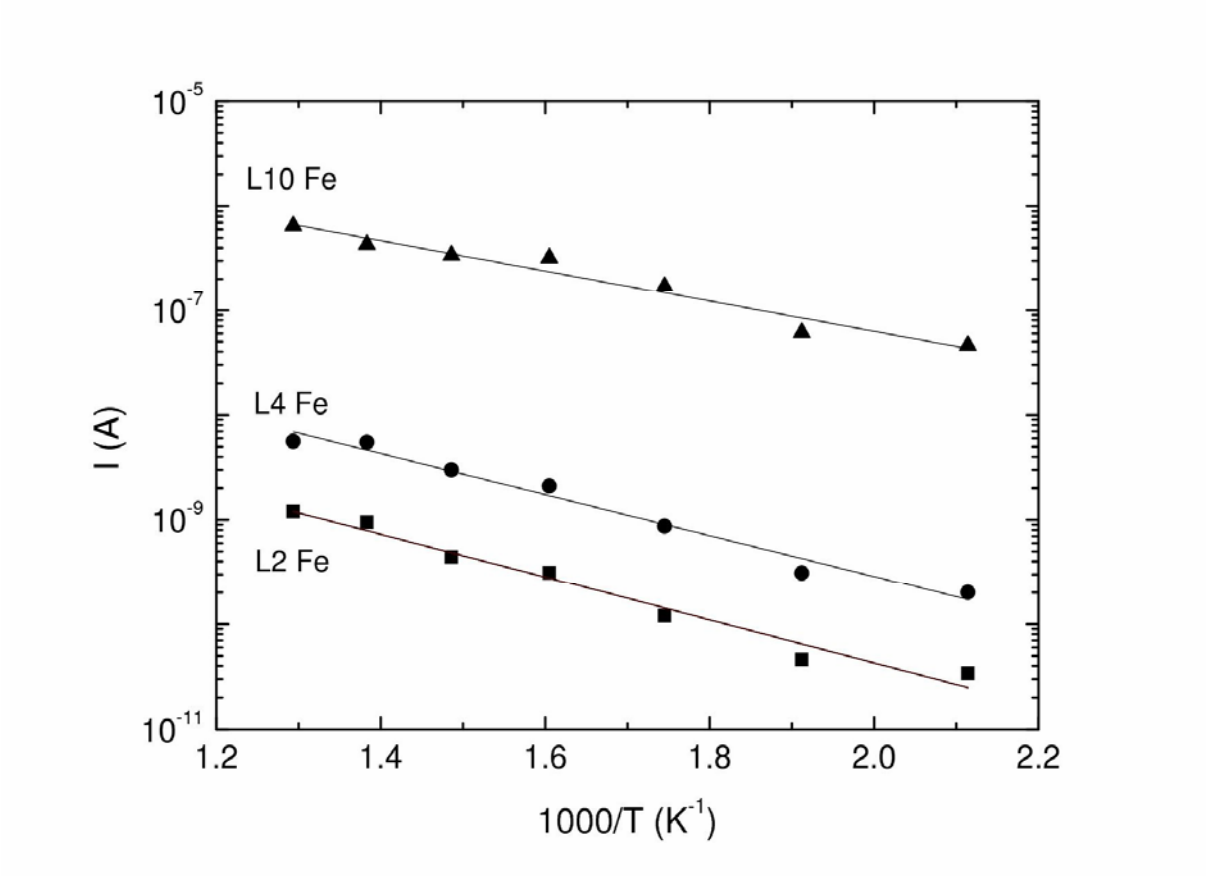

Fig.3: *Arrhenius plot of sensor current I vs. inverse temperature 1/T for Fe_3O_4 LB deposits with M = 2, 4 and 10 NP layers.*

4. Discussion

Conductivity in granular metals both in dielectric regime with isolated particles dispersed in dielectric continuum and in metallic regime with small dielectric inclusions are

discussed in [9]. In the first case transport is mostly by tunneling and these structures were broadly studied as strain gauges [10]. The second type of structures especially with oxide NPs were not studied so often. We consider here NPs with eventual residua of surfactant and/or barriers created by surface reactions of NPs.

The n to p transition in metallic oxides was observed often and in the case of $CoFe_2O_4$ it was ascribed to the excess of Co (less Fe) and Co2+ to Co3+ hopping [11]. Another explanation could be the reaction of NPs with nitrogen, especially in 1 monolayer Fe_2O_3 sample, supported by the fact that in our sensors fluctuations of current in an erratic way were recorded at the exposure to 100 ppm of NO_2 in dry air.

The E values in n-type Fe_2O_3 samples (Tab. 1) calculated from the dependence I vs. 1/T, are similar to those measured by Caricato et al. [12] in laser deposited Fe_2O_3 films or by Tesfamichael et al. [13] in e-beam deposited WO_3 films. (E values are much smaller than the band gap energy $E_g = 2 – 3$ eV of bulk oxides.) In [12] they were identified with $E_g/2$, in [13] with barrier heights at the grain boundaries. In the first case the resistivity of films was 0.1 Ωcm, being typical for γ-Fe_2O_3 used in magnetic media [14]. In the second case the resistivity is of the order 10^5 Ωcm like in our samples. Therefore we assume that in our NP arrays the resistivity is governed by inter-particle barriers and the intra-particle resistance is temperature independent to the first approximation [13]. However, at temperatures > 350°C also second mechanism characterized by higher activation energy E_1 in samples with p-type conductivity was observed and this may be explained by intra-particle transport, where also size effects are to be considered because NPs are smaller than the typical mean free path (10 nm) of charge carriers in solid state. We tried to straighten the bent curves of p –type samples using I vs. $(1/T)^{1/4}$ representation like it was done with γ-Fe_2O_3 NP composite in [15], assuming variable range hopping transport. But this approach failed. The current (conductivity) of Fe_2O_3 (Fig. 3) and $CoFe_2O_4$ samples increases with M almost exponentially. This hints at the percolation transport and formation of fully interconnected network at 4 or even more monolayers. Altogether, we think, our explanation of the observed phenomena might be plausible.

Acknowledgement
This work was financially supported by Scientific Grant Agency VEGA, grant 2/0162/12, by bilateral CNR – SAS project 2013 – 2015 and by Centre of Excellence SAS FUN – MAT.

References:

[1] M. M. Arafat et al.: Sensors, **12**, 7207 (2012).
[2] S. Luby et al.: Vacuum, **86**, 590 (2012).
[3] S. Luby et al.: Physics Procedia, **32**, 152 (2012).
[4] E. K. Heidari et al.: Sensors and Actators B, **146**, 165 (2010).
[5] N. P. Zaretskij et al.: Sensors and Actuators B, **170**, 148 (2012).
[6] P. Siffalovic et al.: Langmuir, **26**, 5451 (2010).
[7] L. Chitu et al. : Mater. Sci. Engn. C, **27**, 23 (2007).
[8] F. Bertram et al.: J. Appl. Phys. **110**, 102208 (2011).
[9] X. Batlle et at.: J. Phys. D: Appl. Phys., **35**, R 15 (2002).
[10] H. Moreira et al.: Nanotechnology, **24**, 095701 (2013).
[11] X. Chu. et al.: Sensors and Actuators B, **120**, 177 (2006).
[12] A. P. Caricato et al.: J. Phys. D:Appl. Phys, **40**, 4866 (2007).
[13] T. Tesfamichael et al.: Sensors and Actuators B, **168,** 345 (2012).
[14] T. Doi et al.: US patent 6165608.
[15] Z. Guo et al.: J. Nanopart. Res., **11**, 1441 (2009).